

## Erratum: New physics and tau $g-2$ using LHC heavy ion collisions [Phys. Rev. D **102**, 113008 (2020)]

Lydia Beresford and Jesse Liu

(Received 19 July 2022; published 10 August 2022)

DOI: [10.1103/PhysRevD.106.039902](https://doi.org/10.1103/PhysRevD.106.039902)

This Erratum reports and corrects a bug found in the code that converts the Wilson coefficient  $C_{\tau B}$  to  $\delta a_\tau$  and  $\delta d_\tau$ . The conversion is correctly printed in Eq. (4) of our paper; however, a bug in the code erroneously set the electron charge to unity rather than the correct  $1/\sqrt{4\pi}$  in Heaviside-Lorentz units. This led to  $\sqrt{4\pi} \simeq 3.5$  times faster cross-section variations as a function of  $\delta a_\tau$  and  $\delta d_\tau$ . In Figs. 1 (left and center), 2–5, and Table I, we correct the  $\delta a_\tau$  and  $\delta d_\tau$  values by this flat factor of  $\sqrt{4\pi}$  to fix the error. These replace Figs. 2 (left and center), 3, 5, 6, 7, and Table I in the paper, respectively.

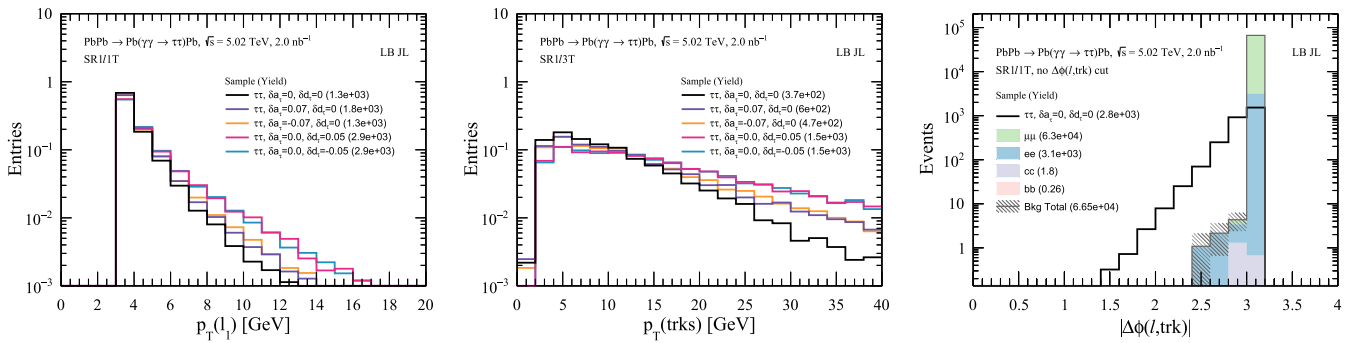


FIG. 1. Distributions of lepton  $p_T$  in SR1 $\ell$ 1T (left) and the 3-track system  $p_T$  in SR1 $\ell$ 3T (center) for benchmark signals with various  $\delta a_\tau$ ,  $\delta d_\tau$  couplings. These are normalized to unit integral to illustrate shape changes with varying  $\delta a_\tau$ ,  $\delta d_\tau$ . The lepton-track azimuthal angle  $|\Delta\phi(\ell, \text{trk})|$  in SR1 $\ell$ 1T (right) is shown for backgrounds (filled) and signal  $\delta a_\tau = \delta d_\tau = 0$  (line), illustrating powerful discrimination against dilepton processes.

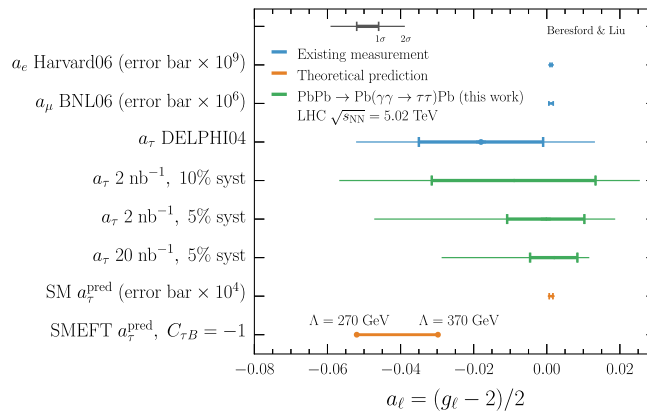


FIG. 2. Summary of lepton anomalous magnetic moments  $a_\ell = (g_\ell - 2)/2$ . Existing single-experiment measurements of  $a_e$  [1],  $a_\mu$  [2], and  $a_\tau$  [3] are in blue. Our benchmark projections (green) assume  $2 \text{ nb}^{-1}$  and  $20 \text{ nb}^{-1}$  for 5% and 10% systematic uncertainties. For visual clarity, we inflate  $1\sigma$  error bars on  $a_e$  ( $a_\mu$ ) measurements by  $10^9$  ( $10^6$ ), and  $10^4$  for the SM prediction  $a_\tau^{\text{pred}}$  (orange) [4]. Collider constraints have thick (thin) lines denoting 68% C.L.,  $1\sigma$  (95% C.L.,  $\sim 2\sigma$ ). The SMEFT predictions [5,6] from Eq. (4) of the paper with  $C_{\tau B} = -1$  displays BSM scales  $270 < \Lambda < 370 \text{ GeV}$  (thick orange).

Published by the American Physical Society under the terms of the [Creative Commons Attribution 4.0 International license](https://creativecommons.org/licenses/by/4.0/). Further distribution of this work must maintain attribution to the author(s) and the published articles title, journal citation, and DOI.

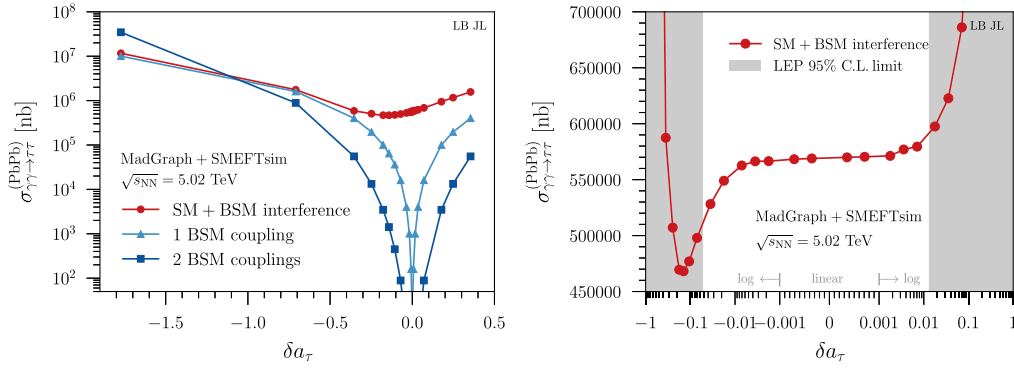


FIG. 3. Generator level cross sections for  $\gamma\gamma \rightarrow \tau\tau$  sourced by our implementation of the Pb photon flux in MadGraph. This is interfaced with SMEFTsim for BSM coupling variations in  $\delta a_\tau$  defined in Eq. (4) of the paper, fixing  $\delta d_\tau = 0$  at  $\sqrt{s_{\text{NN}}} = 5.02$  TeV. Left: contribution from only 1 BSM coupling (light blue triangles), 2 BSM couplings (dark blue squares), and their combined interference with the SM (red circles). The markers indicate the sampled points from  $\delta a_\tau$ . Right: closeup of the  $\delta a_\tau$  values near zero with gray regions denoting the 95% C.L. exclusion by DELPHI, where the horizontal axis is linear scale for  $\delta a_\tau \in [-0.001, 0.001]$  and logarithmic elsewhere.

Figure 1 (right) is unaffected by the conversion error; however, we clarify the y-axis label to be “Events” rather than “Events/0.20”; this figure replaces Fig. 2 (right) in the paper. We note a further clarification: when requiring exactly one lepton plus track(s) in the definition of the signal regions, muons and electrons with transverse momentum down to 0.5 GeV are utilized and tracks with transverse momentum down to 0.1 GeV are utilized; this was not stated in the paper.

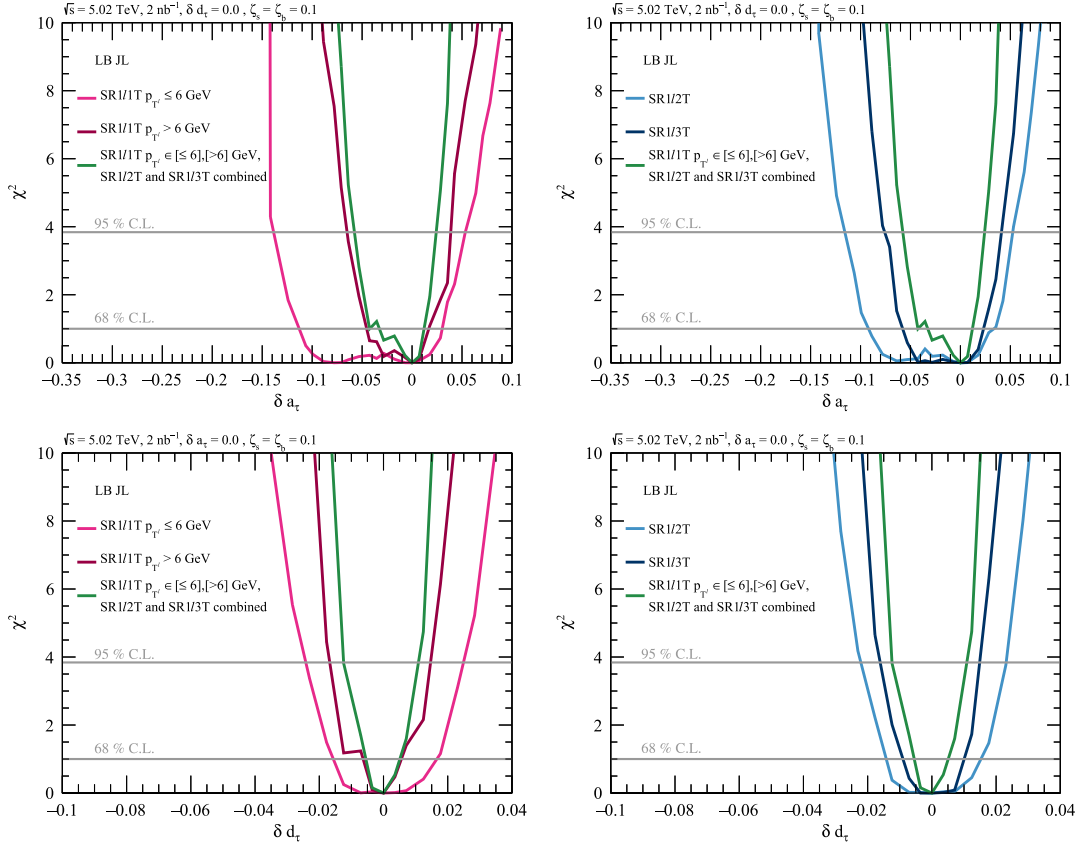


FIG. 4. The  $\chi^2$  distributions as a function of  $\delta a_\tau$  assuming  $\delta d_\tau = 0$  (upper), and  $\delta d_\tau$  assuming  $\delta a_\tau = 0$  (lower) are displayed for 10% systematics at  $\mathcal{L} = 2 \text{ nb}^{-1}$ . Left: results from the SR1 $\ell$ 1T regions and the impact of binning in  $p_{T_\tau}^\ell$ . Right: results from the SR1 $\ell$ 2/3T regions. The four signal region combined  $\chi^2$  is shown by the green line for reference. The gray horizontal lines correspond to 68% C.L. ( $\chi^2 = 1$ ) and 95% C.L. ( $\chi^2 = 3.84$ ). The unphysical spikes are due to limited MC statistics.

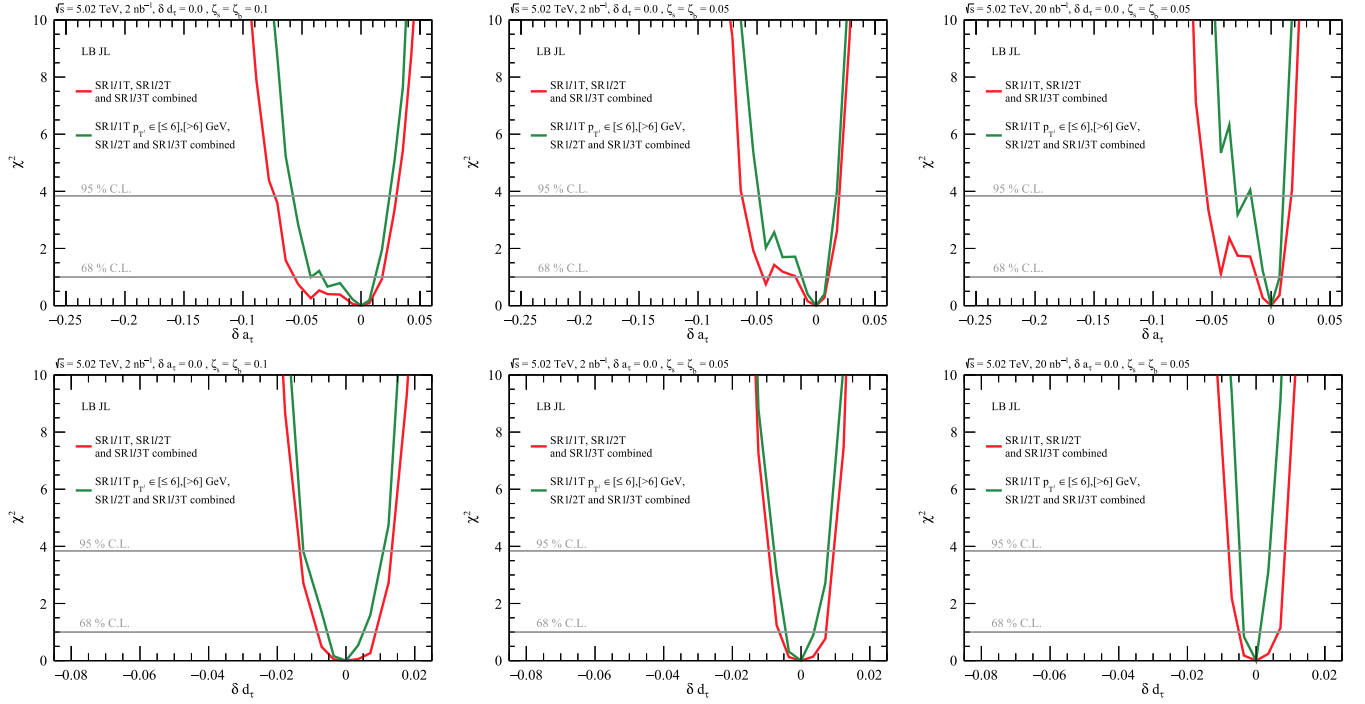


FIG. 5. The  $\chi^2$  distributions as a function of  $\delta a_\tau$  assuming  $\delta d_\tau = 0$  (upper), and  $\delta d_\tau$  assuming  $\delta a_\tau = 0$  (lower). These are displayed for 10% (left), 5% (center) systematics at  $\mathcal{L} = 2 \text{ nb}^{-1}$ , and 5% systematics result extrapolated to  $\mathcal{L} = 20 \text{ nb}^{-1}$  (right). The combined  $\chi^2$  for all three track SRs is shown by the red line, while the impact of dividing SR1 $\ell$ 1T into two orthogonal  $p_T^\ell$  bins is shown by the green line. The gray horizontal lines correspond to 68% C.L. ( $\chi^2 = 1$ ) and 95% C.L. ( $\chi^2 = 3.84$ ). The unphysical spikes are due to limited MC statistics.

TABLE I. Cutflow of event yields after each requirement applied sequentially, normalized to  $\mathcal{L} = 2 \text{ nb}^{-1}$  for the different analyses. For the  $\gamma\gamma \rightarrow \tau\tau$  signal processes, we show these for benchmark points with parameter values labeled by  $(\delta a_\tau, \delta d_\tau)$  displayed in the column header. Backgrounds are shown for various dilepton  $\mu\mu$ ,  $ee$ , and diquark where the letters denote the flavor. The initial value in each cutflow is the cross-section  $\sigma$  times luminosity  $\mathcal{L}$ , followed by the efficiency  $\epsilon_{\text{filter}}$  of the filter applied at generator level to the  $\gamma\gamma \rightarrow \tau\tau$  samples.

Requirement	$\tau\tau(0, 0)$	$\tau\tau(0.018, 0)$	$\tau\tau(-0.035, 0)$	$\mu\mu$	$ee$	$bb$	$cc$	$ss$	$uu$	$dd$
1 lepton + 1 track analysis (SR1 $\ell$ 1T)										
$\sigma \times \mathcal{L}$	1139800	1195060	1056400	844080	844080	2999	604080	37754	604080	37754
$\sigma \times \mathcal{L} \times \epsilon_{\text{filter}}$	241140	253920	226300	844080	844080	2999	604080	37754	604080	37754
1 $\ell$ plus 1 track	20492.2	21619.3	19348.4	263443	3299.3	5.4	2905.0	0.3	5.4	0.2
$p_T^{e/\mu} > 4.5/3 \text{ GeV}$ , $ \eta^{e/\mu}  < 2.5/2.4$	3659.9	3882.7	3582.8	79043	3118.9	1.1	4.8	0.0	0.0	0.0
$p_T^{\text{trk}} > 0.5 \text{ GeV}$ , $ \eta^{\text{trk}}  < 2.5$	3324.5	3535.9	3256.9	78973	3117.8	1.0	3.0	0.0	0.0	0.0
$ \Delta\phi(\ell, \text{trk})  < 3$	1519.7	1605.7	1468.3	0.9	5.3	0.7	1.8	0.0	0.0	0.0
$m_{\ell, \text{trk}} \notin \{[3, 3.2], [9, 11]\} \text{ GeV}$	1275.1	1353.6	1242.3	0.9	5.3	0.2	1.2	0.0	0.0	0.0
$p_T^\ell \leq 6.0 \text{ GeV}$	1197.7	1262.3	1154.7	0.9	0.0	0.2	1.2	0.0	0.0	0.0
$p_T^\ell > 6.0 \text{ GeV}$	77.3	91.3	87.6	0.0	5.3	0.0	0.0	0.0	0.0	0.0
1 lepton + multitrack analysis (SR1 $\ell$ 2/3T)										
$\sigma \times \mathcal{L}$	1139800	1195060	1056400	844080	844080	2999	604080	37754	604080	37754
$\sigma \times \mathcal{L} \times \epsilon_{\text{filter}}$	241140	253920	226300	844080	844080	2999	604080	37754	604080	37754
1 $\ell$ plus 2 or 3 tracks	5945.1	6260.1	5572.2	33.8	23.2	43.8	8056.6	5.4	132.9	6.8
$p_T^{e/\mu} > 4.5/3 \text{ GeV}$ , $ \eta^{e/\mu}  < 2.5/2.4$	1010.0	1073.3	978.6	12.2	4.2	1.8	13.3	0.0	0.0	0.0
$\ell + 2$ tracks, $p_T^{\text{trk}} > 0.5 \text{ GeV}$ , $ \eta^{\text{trk}}  < 2.5$	519.9	548.1	485.8	5.6	4.2	0.8	4.8	0.0	0.0	0.0
$\ell + 3$ tracks, $p_T^{\text{trk}} > 0.5 \text{ GeV}$ , $ \eta^{\text{trk}}  < 2.5$	370.5	398.3	381.1	0.0	0.0	0.4	3.6	0.0	0.0	0.0

As shown in Fig. 2, after the bug fix and assuming the current dataset  $\mathcal{L} = 2 \text{ nb}^{-1}$  with 10% systematics, we find  $-0.031 < a_\tau < 0.013$  at 68% C.L. Prospects assuming halved systematics give  $-0.011 < a_\tau < 0.010$  (68% C.L.). A tenfold dataset increase assumed for the High-Luminosity LHC (HL-LHC) reduces this to  $-0.0046 < a_\tau < 0.0083$  (68% C.L.). The orange line in Fig. 2 shows  $270 < \Lambda < 370 \text{ GeV}$ , where our  $20 \text{ nb}^{-1}$ , 5% systematics proposal has 95% C.L. sensitivity, surpassing DELPHI by 100 GeV. Our projected 95% C.L. sensitivity on  $d_\tau = (e/m_\tau)\delta d_\tau$  is  $|d_\tau| < 1.2 \times 10^{-16} e \text{ cm}$ , assuming  $\delta a_\tau = 0$  with  $2 \text{ nb}^{-1}$ , 10% systematics. Note that the bug only affects BSM variations and does not impact the SM cross section. Although fixing this bug quantitatively changes our results, qualitatively the physics message is unchanged: the analyses proposed in the paper utilizing LHC heavy-ion collisions remains an innovative and promising way to surpass existing lepton collider precision on  $a_\tau$ , opening novel avenues to new physics, and should therefore be pursued experimentally by the LHC collaborations.

- [1] B. Odom, D. Hanneke, B. D’Urso, and G. Gabrielse, New Measurement of the Electron Magnetic Moment Using a One-Electron Quantum Cyclotron, *Phys. Rev. Lett.* **97**, 030801 (2006).
- [2] G. W. Bennett *et al.* (Muon g-2 Collaboration), Final report of the Muon E821 anomalous magnetic moment measurement at BNL, *Phys. Rev. D* **73**, 072003 (2006).
- [3] J. Abdallah *et al.* (DELPHI Collaboration), Study of tau-pair production in photon-photon collisions at LEP and limits on the anomalous electromagnetic moments of the tau lepton, *Eur. Phys. J. C* **35**, 159 (2004).
- [4] S. Eidelman and M. Passera, Theory of the tau lepton anomalous magnetic moment, *Mod. Phys. Lett. A* **22**, 159 (2007).
- [5] R. Escribano and E. Masso, New bounds on the magnetic and electric moments of the tau lepton, *Phys. Lett. B* **301**, 419 (1993).
- [6] B. Grzadkowski, M. Iskrzynski, M. Misiak, and J. Rosiek, Dimension-six terms in the standard model Lagrangian, *J. High Energy Phys.* **10** (2010) 085.